Efficient Light Field Computation for View Range Expansion Using Viewpoint Reduction

Jianhong Han
Institute of Computer Science and Technology
Peking University

Ke Wang
Institute of Computer Science and Technology
Peking University

Jie Feng*
Institute of Computer Science and Technology
Peking University

Bingfeng Zhou
Institute of Computer Science and Technology
Peking University

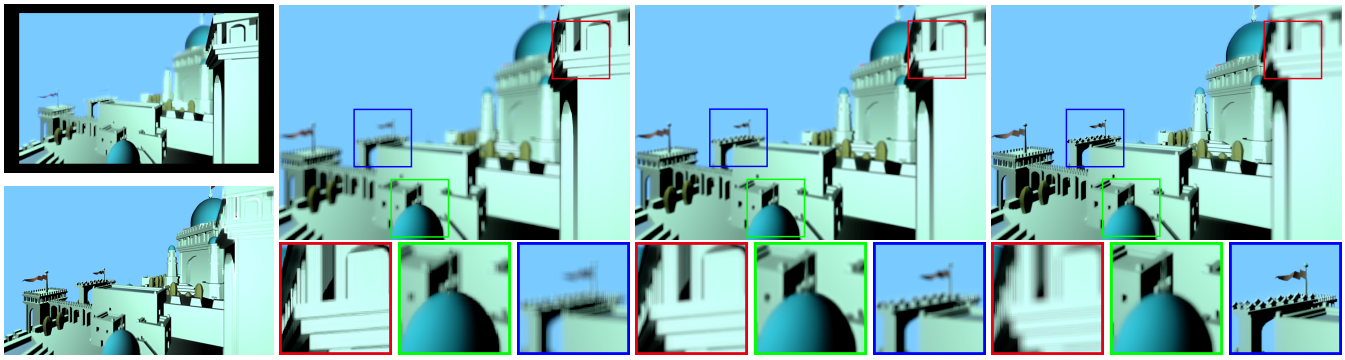

Figure 1: Light field display with different focus. Factored patterns for displaying on LCDs are shown in the left column. The simulated results (right columns) are obtained by focusing on the scene of the 4D light field with a virtual camera.

ABSTRACT

In this paper, we present an improved light field display method with wider view range. In our system, two stacked transparent LCDs are used for glasses-free light field display. They modulate the uniform backlight which enters the observer's eyes to approximate the desired light field. The patterns displayed on the LCDs are optimized according to the target light field using an algorithm based on nonnegative matrix factorization (NMF). In order to achieve wider view range and reduce the computational complexity of the pattern optimization, we utilize a small number of sampling views of the light field. To properly choose the subset of the sampling views, a stochastic sampling algorithm is adopted. The effectiveness of the proposed method is demonstrated by the experimental results, and similar light field display results can be generated with reduced sampling views.

CCS CONCEPTS

• **Computing methodologies** → **Virtual reality**; • **Hardware** → *Displays and imagers*;

KEYWORDS

light field display, computational photography, nonnegative matrix factorization, stochastic sampling

ACM Reference Format:
Jianhong Han, Ke Wang, Jie Feng, and Bingfeng Zhou. 2018. Efficient Light Field Computation for View Range Expansion Using Viewpoint Reduction. In *SIGGRAPH Asia 2018 Technical Briefs (SA '18 Technical Briefs), December 4–7, 2018, Tokyo, Japan.* ACM, New York, NY, USA, 4 pages. https://doi.org/10.1145/3283254.3283267

*Corresponding author. Email: feng_jie@pku.edu.cn .

SA '18 Technical Briefs , December 4–7, 2018, Tokyo, Japan

ACM ISBN 978-1-4503-6062-3/18/12…$15.00
https://doi.org/10.1145/3283254.3283267

1 INTRODUCTION

Early virtual reality (VR) devices can provide immersive 3D experience. However, they may also cause visual fatigue after being used for a few more moments. The reason is that these virtual reality devices do not produce a natural three-dimensional scene, and that may cause the vergence-accommodation conflict. Furthermore, they often employ highly complex geometry models for 3D scenes, which are expensive for practical application.

Light field is a method of recording all the light in the scene. When a light field is restored to the observer's eyes, the real scene can be simulated to achieve the effect of refocusing and free viewpoint, and the feeling of dizziness caused by VR devices can be reduced or even eliminated. Meanwhile, it avoids the complexity of traditional geometric modeling, and hence has great advantages in VR, computational photography and other applications. Levoy and Hanrahan [1996] introduced the concept of 4D light field into computer graphics. According to this concept, the target light field for display can be described by two planes: a scene plane and a pupil plane. When observing the light field, the pupil is free to move within a limited range, here we call it the *view range*. For

convenience of calculation, the view range is discretized into a set of *viewpoints*. Hence, all the light rays received at a viewpoint from the scene plane constitute a 2D image, namely a *sampling view*.

The methods of light field acquisition have been relatively mature. The devices utilized in light field acquisition include handheld camera [Shi et al. 2014], and light field cameras based on camera array [Wilburn et al. 2005] or lens array [Levoy et al. 2006]. When the light field is obtained, it can be rendered to generate new images of the scene at different viewpoints with different focus depth.

Light field display is more difficult and not fully developed. According to different types of devices, light field display techniques can be roughly divided into glasses-free 3D display and head-mounted display. Glasses-free 3D displays usually employ muti-projector arrays [Matusik and Pfister 2004] or multilayer LCDs [Lanman et al. 2011; Wetzstein et al. 2012]. Unfortunately, these display devices are often heavy and expensive. The head-mounted display devices can produce a near-eye stereoscopic display effect, and generally provide a wider field of view. [Lanman and Luebke 2013] implemented near-eye light field display by micro-lens arrays. Light field stereoscope system [Huang et al. 2015] used cascaded convex lenses and LCDs. These systems are usually driven by algorithms such as computed tomography, nonnegative matrix factorization [Lanman et al. 2011] and nonnegative tensor factorization [Wetzstein et al. 2012]. However, they have great challenges in view range, resolution and display accuracy.

In this paper we propose a method for light field display optimization using dual LCDs and view range expansion. According to prior researches, a 4D light field can be reconstructed from a properly selected subset of 2D sample images, utilizing the sparsity in the frequency domain of light fields. In similar way, by downsampling the viewpoints used in light field construction, the computational cost can be reduced substantially. Hence, with the same computational cost, a larger view range is possible to be calculated. In this sense, we may expand the view range in light field display. A blue-noise stochastic sampling algorithm is adopted to obtain better viewpoint distribution. We validate the effectiveness of our approach with a hardware prototype and camera simulation.

2 WIDE-RANGE LIGHT FIELD DISPLAY

Our prototype has a similar setup with the light field stereoscope method [Huang et al. 2015]. It adopts two stacked LCDs and a magnifying lens to simulate a light field. The original system is proposed for near-eye light field display and can produce nearly correct focus cues. However, its view range is too limited for glasses-free light field display. Hence, we aim to improve the method, to provide a wider view range. For this purpose, we utilize the sparsity of 4D light field to expand the view range.

2.1 Light Field Display based on NMF

As shown in the Fig.2, our display system consists of a convex lens and two stacked LCDs. Two patterns are calculated according to a target light field, and displayed respectively on the two LCDs, acting as a modulation array. The LCD close to the lens is transparent, the rear one is opaque with backlight. The uniform backlight is modulated by the LCDs in a multiplicative manner, reaches the observer's eye through the convex lens, and generates a virtual and

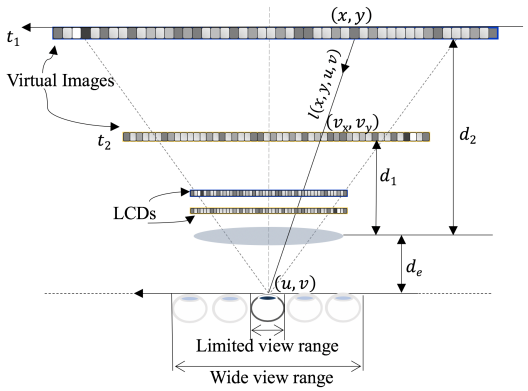

Figure 2: The light field display system adopts two stacked LCDs and a convex lens. The LCDs modulate the uniform backlight to simulate the target light field.

magnified view of the target light field. Therefore, our optimization target is to adjust the two patterns until the displayed light field is close to the target one.

Each ray $l(x, y, u, v)$ in the scene can be described by the corresponding pixels on the virtual images of the two patterns on the LCDs. According to the spatial similarity, l can be formulated as:

$$\begin{aligned} l(x, y, u, v) &= t_1(x, y) t_2(v_x, v_y) \\ &= t_1(x, y) t_2(x - \frac{(x-u)(d_2-d_1)}{d_2+d_e}, y - \frac{(y-v)(d_2-d_1)}{d_2+d_e}). \end{aligned} \tag{1}$$

Here, the virtual images of the display patterns are denoted as t_1 and t_2 respectively. The ray passes through t_1 at (x, y), through t_2 at (v_x, v_y), and reaching the pupil plane at (u, v).

By discretizing and vectorizing Eq.1, we formulate the 4D light field following [Huang et al. 2015]:

$$\widetilde{\mathbf{l}} = \Phi_1 t_1 \circ \Phi_2 t_2, \tag{2}$$

where $\circ$ is Hadamard product. The sparse matrices Φ_1 and Φ_2 are mapping functions used to determine the intersection of light rays with the virtual images. Therefore, the light field can be reconstructed by solving the following optimization problem:

$$\underset{\{t_1, t_2\}}{\text{minimize}} \left\| \beta \mathbf{l} - \widetilde{\mathbf{l}} \right\|_2^2. \tag{3}$$

Here, $\mathbf{l}$ is the vectorized form of the target light field. It contains a group of 2D sample images of the light field, which can be achieved by light field cameras or rendered by ray tracing. β is a user-defined brightness coefficient. The non-negativity constraints ensure that optimized patterns are logically feasible. This problem can be solved in an alternating and iterative fashion using multiplicative update rules [Blondel et al. 2007]. The rule for t_1 is:

$$t_1 \leftarrow t_1 \circ \frac{\Phi_1^T(\beta \mathbf{l} \circ (\Phi_2 t_2))}{\Phi_1^T(\widetilde{\mathbf{l}} \circ (\Phi_2 t_2)) + \epsilon}, \tag{4}$$

and similar for t_2. In this way, the display patterns t_1 and t_2 can be solved through the optimization.

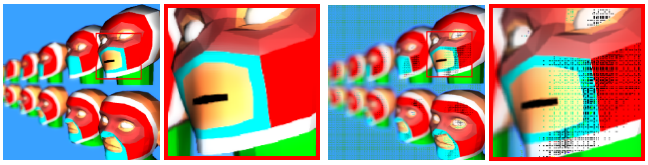

5 × 5 Viewpoints 11 × 11 Viewpoints

Figure 3: Display result of brutally expanding view range. Zero pixels may appear due to optimization failure.

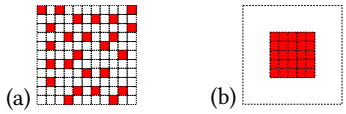

Figure 4: Viewpoints used for light field pattern optimization. (a) Stochastic sampling viewpoints in a larger view range. (b) Full sampling viewpoints in a small view range.

Obviously, the time cost of target light field sampling is mostly dependent on the geometric complexity of the scene and the number of viewpoints, while the time for light field factorization only depends on the latter.

2.2 Expanding View Range of Light Filed Display

When calculating the display patterns on the two LCDs, existing methods have strong constraints on the view range and the number of viewpoints. However, in practical application, one may need to observe the light field in a larger view range. Thus more viewpoints and rays need to be considered in light field pattern optimization. If we directly expand the view range and perform light field sampling and pattern optimization on a large number of viewpoints, the time cost will grow quadratically. Moreover, that may also lead to decline in display quality, or even convergence failure, as shown in Fig.3. In fact, the amount of rays involved in the calculation is determined both by the resolution of the LCD screen and the number of viewpoints on the pupil plane. Obviously, reducing the resolution of the LCDs would decrease the quality of display. Therefore we can only reduce the number of sampling viewpoints in the pupil plane to decrease the amount of rays.

The light field itself has a lot of redundancy. Shi et al. [2014] utilized the sparsity of the continuous Fourier spectrum, and reconstructed a 4D light field from only a small number of sampling images. In fact, the light field is sparse not only in frequency domain but also in spatial domain, reflected as that the light emitted from the same point in the scene has similar color at most of the viewpoints. Therefore, we may obtain approximate display results by reducing the number of sampling viewpoints.

In order to get more stable and accurate convergence results, we need to choose an appropriate subset of viewpoints. A series of commonly used sampling methods are tested, including regular sampling, circular sampling, diagonal sampling, etc. Through experiments, we find that the light field obtained by stochastic sampling is superior to others in terms of quality and isotropy. Hence, to get a better viewpoint distribution, we adopt an error-diffusion sampling method with blue-noise property [Zhou and Fang 2003]. This method is able to make the sampling distribution more uniform,

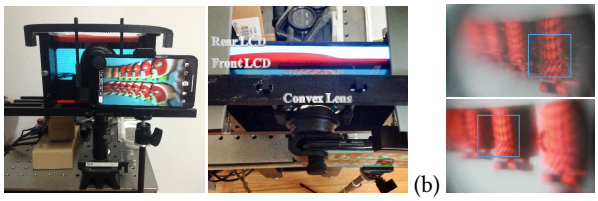

(a) (b)

Figure 5: (a) The setup of our hardware prototype. (b) The light field display results captured by a camera (top: front focus; bottom: rear focus).

isotropic, and the number of samples is controllable. As demonstrated in Fig.4, in a view range consisting of 11 × 11 viewpoints, 25 viewpoints are selected to participate the optimization, while with traditional methods, 25 samples can only support a view range of 5 × 5 viewpoints. In another word, using the same number of viewpoints in the optimization, which means the same amount of calculation, our method can obtain wider view range. Experimental results demonstrate the effectiveness.

3 EXPERIMENTAL RESULTS

We implement the proposed light field optimization and view expansion method, obtaining satisfying display results on both hardware prototype and simulation system.

3.1 Hardware Prototype

The system consists of two cascaded LCDs and a convex lens (Fig.5(a)). The resolution of both LCDs is 1280 × 800 pixels, and the size is $14.976cm \times 9.36cm$. The focal length of the convex lens is $f = 5cm$. The diameter of the lens is $6cm$. The front LCD is $3.8cm$ away from the lens, and the rear one is $4.8cm$ away. The distance of two adjacent discretized viewpoints in the view range is $1mm$.

Fig.5(b) gives an example of refocusing effect in light field display. When using the zooming of a camera to simulate the focusing of human eyes, our prototype can produce correct refocusing effects.

3.2 Software Simulation

Since the display precision of current hardware prototype is not high enough, we also develop a software simulating system to more precisely verify the effect of refocusing and free viewpoint. Here, the parameters of the simulating system are set the same as the hardware prototype.

A virtual camera is set up in the system. In this camera model, the relationship between the object distance d and the image distance d' can be formulated by the Gaussian thin lens equation. Therefore, when the light rays emitted from the scene pass through the lens, they will converge at one point ($d = f$) or diffuse as a spot ($d \neq f$) on the image plane (see the supplementary for the schematics). In this way, we can simulate the image generated in human eyes when focusing on the scene that represented by the displayed light field.

By adjusting the focal length f of the virtual camera, we can calculate projection images at different focusing depth. For the experimental results in this paper (Fig.1, 5(b), 6, 7(top), 8, 9), the view range of the light field consists of 11 × 11 viewpoints, and 25 sampling viewpoints are used in optimization, as in Fig.4(a). Objects present a clear image when they are on the focal plane, otherwise present a blurred image. The results show that the light field can be

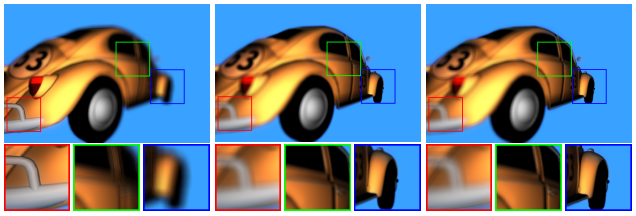

Front Focus Mid Focus Rear Focus

Figure 6: Simulated display results of light field reconstructed with selected sample views (Fig.4(a)). The scene can be refocused dynamicly.

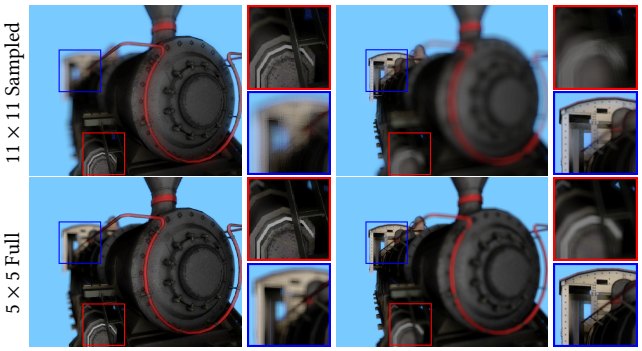

Figure 7: Simulated display results comparison of light field reconstructed with sampled and full viewpoints (Fig.4).

simulated by the stacked LCDs, and the 4D light field reconstructed by our method allow the observer to refocus within the scene.

In Fig.7, we compare the light field simulation results with a small full-sampled view range and an expanded downsampled view range. The results show that in both cases, the refocusing effect at different depths and image quality in focused areas are similar. However, after viewpoint downsampling, the image quality in unfocused area is degraded. Inevitably, downsampling will cause losses, but we can balance the display quality and the amount of calculation by controlling the number of samples.

Fig.8 demonstrates that, at non-sampling viewpoints, light field can also be correctly simulated, although the original information is not fully recorded. The display results are close to the reference view generated by ray tracing at the same viewpoint.

Because the view range is enlarged, we can observe the scene from more viewpoints. Therefore, some occluded objects that were previously invisible, may become possible to be observed. Fig.9 gives an example from different viewpoints. The rear left leg is occluded on the left, while the same leg is observed on the right.

4 CONCLUSIONS AND FUTURE WORK

In this paper, we adopt a light field display system based on dual LCDs. In order to expand the view range in light field display and reduce the cost of calculation, we use a small number of selected viewpoints instead of full viewpoints during the display pattern optimization. Experimental results demonstrate that the approximate light fields have satisfying display effect.

There still are some problems, such as the degraded image quality in the unfocused area, and the slight fuzziness at middle depth. Thus

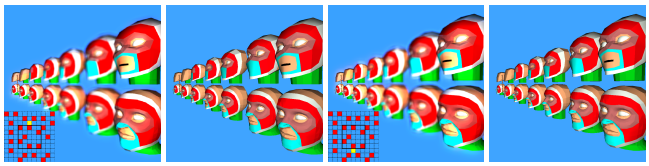

Display Result Reference View Display Result Reference View

Figure 8: Display results synthesized by the display patterns at a non-sampling viewpoint using our method. The yellow marker shows the position of viewpoint.

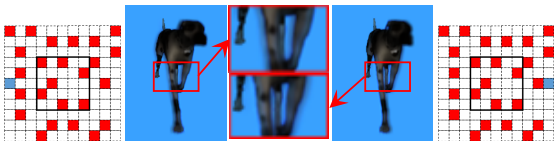

Figure 9: Rendering results from two different viewpoints of the same scene. Larger view range makes it possible to produce different occlusion.

we will search for better sampling methods and post-processing method such as smoothing. Also, two LCDs cannot meet the requirements of all light displaying at the same time. Therefore, adding more LCDs may improve the display ability. Time-multiplexed image display will also be considered to provide even larger view range. Hardware prototype will be improved to be applied to practical application.

ACKNOWLEDGMENTS

This work was supported by National Natural Science Foundation of China #61602012 and National Key Research and Development Program of China #2016QY02D0304.

REFERENCES

Vincent D. Blondel, Ngoc diep Ho, and Paul van Dooren. 2007. Weighted nonnegative matrix factorization and face feature extraction. In *Image and Vision Computing*. 1–17.

Fu-Chung Huang, Kevin Chen, and Gordon Wetzstein. 2015. The Light Field Stereoscope: Immersive Computer Graphics via Factored Near-eye Light Field Displays with Focus Cues. *ACM Trans. Graph.* 34, 4, Article 60 (July 2015), 60:1–60:12 pages. https://doi.org/10.1145/2766922

Douglas Lanman, Matthew Hirsch, Yunhee Kim, and Ramesh Raskar. 2011. Content-adaptive parallax barriers: optimizing dual-layer 3D displays using low-rank light field factorization. *ACM Trans. Graph.* 29, 6 (2011), 81–95.

Douglas Lanman and David Luebke. 2013. Near-eye Light Field Displays. In *ACM SIGGRAPH 2013 Emerging Technologies (SIGGRAPH '13)*. ACM, New York, NY, USA, Article 11, 1 pages. https://doi.org/10.1145/2503368.2503379

Marc Levoy and Pat Hanrahan. 1996. Light field rendering. In *Conference on Computer Graphics and Interactive Techniques*. II–64 – II–71.

Marc Levoy, Ren Ng, Andrew Adams, Matthew Footer, and Mark Horowitz. 2006. Light field microscopy. *ACM Trans. Graph.* 25, 3 (2006), 924–934.

Wojciech Matusik and Hanspeter Pfister. 2004. 3D TV: A Scalable System for Real-time Acquisition, Transmission, and Autostereoscopic Display of Dynamic Scenes. *ACM Trans. Graph.* 23, 3 (Aug. 2004), 814–824.

Lixin Shi, Haitham Hassanieh, Abe Davis, Dina Katabi, and Fredo Durand. 2014. Light Field Reconstruction Using Sparsity in the Continuous Fourier Domain. *ACM Trans. Graph.* 34, 1, Article 12 (Dec. 2014), 13 pages. https://doi.org/10.1145/2682631

Gordon Wetzstein, Douglas Lanman, Matthew Hirsch, and Ramesh Raskar. 2012. Tensor Displays: Compressive Light Field Synthesis Using Multilayer Displays with Directional Backlighting. *ACM Trans. Graph.* 31, 4 (July 2012), 80:1–80:11.

Bennett Wilburn, Neel Joshi, Vaibhav Vaish, Einoville Talvala, Emilio Antunez, Adam Barth, Andrew Adams, Mark Horowitz, and Marc Levoy. 2005. High performance imaging using large camera arrays. 24, 3 (2005), 765–776.

Bingfeng Zhou and Xifeng Fang. 2003. Improving mid-tone quality of variable-coefficient error diffusion using threshold modulation. *ACM Trans. Graph.* 22, 3 (July 2003), 437–444. https://doi.org/10.1145/882262.882289